

## Bubble and Ring Formation in Nuclear Fragmentation

Wolfgang Bauer, George F. Bertsch, and Hartmut Schulz

*National Superconducting Cyclotron Laboratory and Department of Physics and Astronomy, Michigan State University,  
East Lansing, Michigan 48824-1321*

(Received 28 May 1992)

Nuclear transport theory predicts the formation of unstable bubbles and rings in the central collision between equal-mass heavy ions. This phenomenon occurs around a beam energy of  $E/A \approx 50$  MeV/nucleon and is due to the compression of the nuclei in the early stage of the collision. As observable consequences, we predict a higher number of intermediate-mass fragments than expected from multifragmentation of a homogeneously filled sphere, and a different pattern of fragment Coulomb accelerations.

PACS numbers: 25.70.Pq, 24.10.Cn

At sufficiently high excitation energies ( $E^*/A \gtrsim 10$  MeV) of nuclear matter, copious production of intermediate-mass fragments is observed. This excitation energy can be deposited in different ways. The two most common are (1) bombardment of heavy target nuclei with very high energy protons [1] (or the same process in reverse kinematics), and (2) central collisions of target and projectile with approximately equal mass numbers at intermediate beam energies ( $E/A \approx 50$  MeV).

The first type of reaction is assumed to be a two-step process. In the first step, the small projectile only interacts with the target nucleons in its direct path; some of the sideways ejected nucleons and pions penetrate into the spectator matter and give rise to its excitation. In the second step, the excited target spectator matter decays.

Central heavy-ion reactions proceed in a different way: In the initial state of the reaction, thermalization takes place via binary nucleon-nucleon collisions. During this stage the nuclei compress each other, whereby typical densities of  $\rho/\rho_0 \approx 1.3-1.5$  are reached. This excited and compressed participant matter then expands and decays.

The reaction mechanism, via which intermediate mass

fragments are formed, is still debated. At lower excitation energies, sequential emission from the surface [2] in a statistical fashion is dominant. At higher energies simultaneous multifragmentation of the entire nuclear volume seems to be favored [3-6]. Since the nuclear interaction exhibits short-range repulsion and intermediate-range attraction, the resulting nuclear equation of state exhibits a phase transition between the liquidlike and gaslike phases. The phenomenon of multifragmentation has been connected to this effect [3,7-9]. Of the phase transition models under consideration so far, percolation based models have been most successful in reproducing high-energy proton-induced and light-ion-induced multifragmentation data [10,11].

In this Letter we propose a novel path leading to the emission of intermediate-mass fragments in heavy-ion collisions: the formation of unstable hollow bubbles and rings of nuclear matter, which decay by fragment emission.

Our reasoning is based on the nuclear Boltzmann-Uehling-Uhlenbeck (BUU) transport theory [12,13], where the transport equation for the nucleonic one-body density distribution function  $f_1 \equiv f(\mathbf{r}_1, \mathbf{p}, t)$  is given by

$$\partial_t f_1 + \frac{\mathbf{p}}{E} \cdot \nabla_{\mathbf{r}} f_1 - \nabla_{\mathbf{r}} U \cdot \nabla_{\mathbf{p}} f_1 = \int d^3 q_1' d^3 q_2 d^3 q_2' \delta(E) \delta^3(\mathbf{p}) \frac{d\sigma}{d\Omega} \{f_1' f_2' (1-f_1)(1-f_2) - f_1 f_2 (1-f_1')(1-f_2')\}. \quad (1)$$

In our numerical implementation [14] we use the test-particle method, in which the solution of Eq. (1) is reduced to the solution of a set of  $6 \times (A_t + A_p) \times N$  coupled first-order differential equations in time, where  $N$  is the number of test particles per nucleon, and  $A_t$  and  $A_p$  are the target and projectile mass numbers, respectively. To reduce artificially created numerical fluctuations due to finite numbers of test particles, we use  $N=1000$  in the present study, leading to a system of  $1.1 \times 10^6$  coupled differential equations in the case of the  $^{93}\text{Nb} + ^{93}\text{Nb}$  system studied below.

The mean-field potential  $U$  appearing in Eq. (1) is parametrized as a density-dependent functional,

$$U(\rho) = A(\rho/\rho_0) + B(\rho/\rho_0)^{4/3}, \quad (2)$$

with the coefficients  $A = -218.1$  MeV and  $B = 164.0$

MeV fixed by nuclear matter saturation properties. This potential yields an incompressibility coefficient  $\kappa = 235$  MeV.

To illustrate the occurrence of the bubble and ring structures, we show in Fig. 1 the time evolution of a central  $^{93}\text{Nb} + ^{93}\text{Nb}$  collision at  $E_{\text{beam}}/A = 60$  MeV. We display the nucleon density in the reaction plane for different times during the reaction. In the initial stage ( $t = 40$  fm/c) of the reaction, the two nuclei compress each other in their overlap zone to a density of  $\rho \approx 1.4\rho_0$ , and the density distribution is approximately spherically symmetric.

The transiently compressed system expands radially, and the central density falls to a value below  $\rho_0/2$ . The bulk of the matter forms a spherical shell.

$^{93}\text{Nb} + ^{93}\text{Nb}$ ,  $E/A = 60$  MeV,  $b = 0$  fm

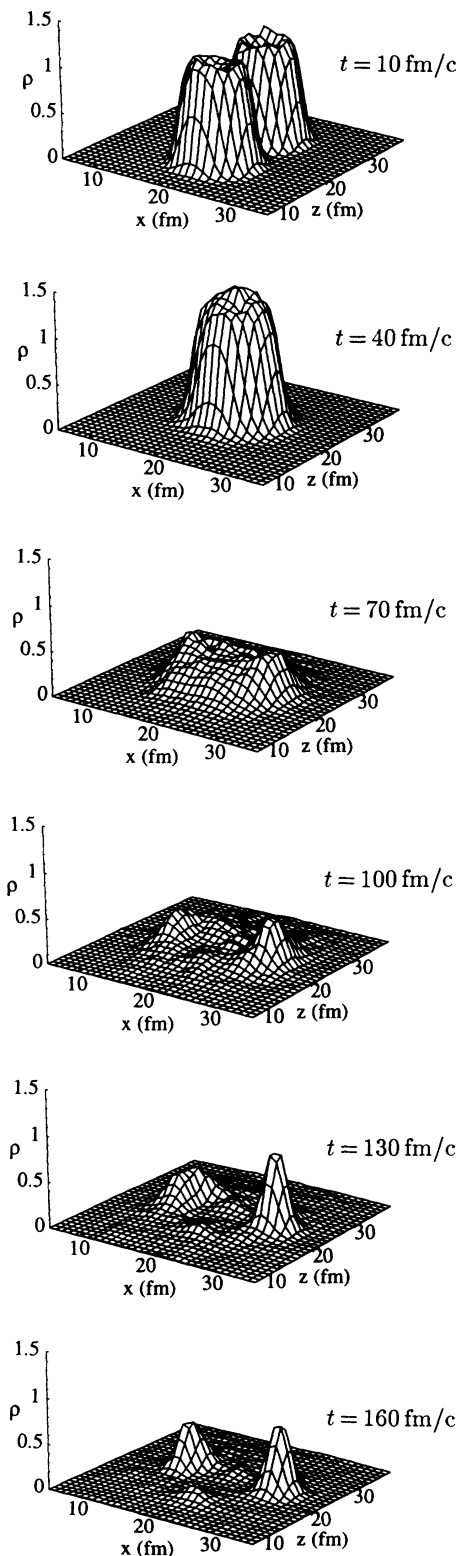


FIG. 1. Calculation of the time evolution of the density  $\rho$  (in units of  $\rho_0$ ) in the reaction plane (the beam axis is in the  $z$  direction) for a central  $^{93}\text{Nb} + ^{93}\text{Nb}$  collision at  $E_{\text{beam}}/A = 60$  MeV.

This behavior may be understood as arising from a delicate balance of several effects. The initial stage gives rise to a spherically symmetric compressed nucleus, if the time to establish local equilibrium is reached just when the nuclei have maximum overlap. Then the subsequent expansion will be mainly radial.

When a compressed sphere expands radially, a rarefaction wave propagates from outside towards the center, leaving matter at normal density streaming outward. When the wave reaches the center, the outward streaming matter depletes the center, sending the density to a low value. At low energies the system slows down and recompresses the hole, but at higher energies, such as we see here, the bubble grows.

What causes the outgoing density wave to stall and enable the formation of a bubble? The matter that forms the outgoing density wave is supplied by the inward propagating rarefaction wave. The continuity equation requires

$$r_{\text{out}}^2 \rho(r_{\text{out}}) v_{\text{out}} = r_{\text{in}}^2 [\rho_c - \rho(r_{\text{in}})] v_{\text{in}} \quad (3)$$

for stationary flow. Here  $r_{\text{in}}, r_{\text{out}}$  and  $v_{\text{in}}, v_{\text{out}}$  are the locations and velocities of the surfaces of the inward and outward propagating wave fronts, respectively. As the rarefaction wave moves in toward the center, the right-hand side of Eq. (3) decreases. As long as there is a well-defined surface with finite density  $\rho(r_{\text{out}})$ , the outflow velocity  $v_{\text{out}}$  must decrease and eventually approach 0. In the case that the radial kinetic energy is large compared to the nuclear binding energy, the outflowing matter vaporizes and Eq. (3) is fulfilled with  $\rho(r_{\text{out}}) \rightarrow 0$ .

In any case, matter close to the center of mass is still streaming outward when the rarefaction reaches the center, and the interior of the nuclear system is depleted of baryon density ( $t = 100\text{--}130$  fm/c). This gives rise to the occurrence of bubble and doughnut like shapes of the density profile.

The occurrence of this striking feature is sensitively dependent on the amount of radial kinetic energy supplied by the initial compression. At higher beam energies, the initial compression is increased, and the energy of radial expansion exceeds the nuclear binding energy. Then the result is a prompt disintegration of the entire nuclear volume. At lower beam energies, the initial compression is too small, and monopole type oscillations are the consequence. Since the initial compression is dependent on the nuclear incompressibility, the occurrence of the shapes predicted by us may also yield valuable information on this key parameter of the nuclear equation of state.

We have conducted studies at several different beam energies and find that for the Nb+Nb system the monopole type oscillation occurs for  $E/A \lesssim 50$  MeV, and that prompt disintegration occurs for  $E/A \gtrsim 80$  MeV. In the energy window between these values bubble and ring formation occurs, even for small nonzero ( $b \lesssim 0.2b_{\text{max}}$ ) im-

compact parameters. We have also studied other symmetric or slightly asymmetric mass systems and find the same effect.

The bubble has a relatively long lifetime despite the occurrence of dynamic instabilities. The onset of these instabilities can be observed from Fig. 2, where we display the square of the sound velocity  $v_s^2$  as a function of the reaction time and the distance to the center of mass. Using our above equation of state, it is

$$v_s^2 = \left( \frac{\partial P}{\partial \rho} \right)_S = \frac{1}{m} \left[ \frac{10}{9} \langle E_k(\rho, T) \rangle + A \frac{\rho}{\rho_0} + \frac{4}{3} B \left( \frac{\rho}{\rho_0} \right)^{4/3} \right], \quad (4)$$

where  $\langle E_k(\rho, T) \rangle$  is the average kinetic energy per nucleon.

For  $t \gtrsim 100$  fm/c, dynamical instabilities become apparent ( $v_s^2 < 0$ ). Now the system becomes unstable to small perturbations or fluctuations in the density [15-17]. Such fluctuations can be induced by two-body nucleon nucleon collision [18] or surface instabilities [19].

We can see from Fig. 1 that the bubble shaped nuclear remnant is converted into a ring (or doughnut) shaped object during the subsequent time evolution, as indicated by the two bumps in the density distribution in the reaction plane ( $t = 160$  fm/c). To show the appearance of the doughnut shape more clearly, we display in Fig. 3 the surface of constant nucleon number density,  $\rho(x, y, z) = 0.3\rho_0$ , as a function of the three spatial coordinates for  $t = 160$  fm/c. Now we can clearly observe the doughnut shape perpendicular to the beam direction including the shape fluctuations due to Rayleigh-Taylor surface instabilities.

The doughnut shape reflects an imbalance towards

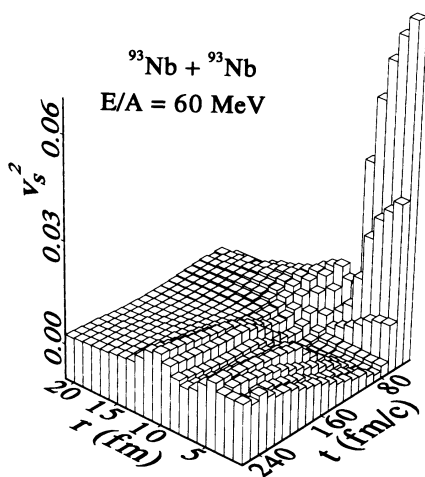


FIG. 2. Calculated square of the local velocity of sound,  $v_s^2$ , as a function of the distance to the center of mass,  $r$ , and the time,  $t$ , for a central  $^{93}\text{Nb} + ^{93}\text{Nb}$  collision at  $E_{\text{beam}}/A = 60$  MeV.

sideways flow in the nearly symmetric compressed phase. The bubble shape would be preserved to longer times for a lighter-mass system, since that would equilibrate slightly later.

From our greatest calculation it cannot be inferred at what time the breakup into fragments occurs. This is outside the scope of the present one-body theory. However, it is clear that the final fragment distribution carries some information of the topology of these intermediate steps shown here.

We predict two major experimental consequences of the bubble and ring formation. First there should be more intermediate-mass fragments formed from these extended systems than would be produced by the decay of a compact object at the same temperature [20]. It is difficult to quantify this tendency, but it is clear that a relatively cool object with a large surface will produce more fragments than a hot object with a smaller surface, which will emit mainly neutrons and hydrogen and helium isotopes. We also expect a difference in the mass distributions between the breakup of rings and bubbles, and we are presently investigating this effect [20].

The second prediction is that the Coulomb acceleration in the final state will on average be smaller than expected from the decay of a uniform density spherical system. Generally, one fits the spectra assuming a distribution of Coulomb barriers as the decay proceeds, and the average barrier will be reduced. If noncompact topological objects are formed transiently, the barrier reduction will be stronger than that from a volume breakup.

There is another small Coulomb effect that may be ob-

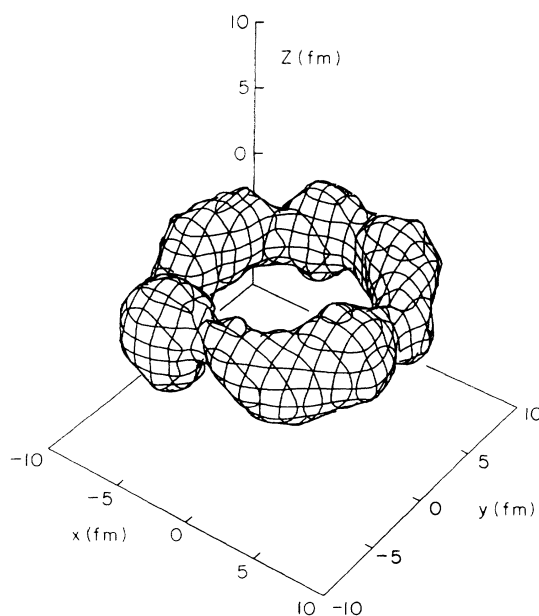


FIG. 3. Surface of constant nucleon number density,  $\rho(x, y, z) = 0.3\rho_0$ , for the same reaction as in Figs. 1 and 2 at  $t = 160$  fm/c.

servable. In volume decays, a small fraction of the fragments originate at the center and are not subject to Coulomb acceleration. This fraction will no longer be present here, because the center is empty. All the fragments are at roughly a common radius.

In summary, we predict the occurrence of bubbles and rings of nuclear matter for central heavy-ion collisions at beam energies per nucleon around 50–60 MeV. The bubble shape we find is similar to the one observed by using a spherically symmetric, compressed, and heated nuclear system as an initial condition and propagating it via the time-dependent Hartree-Fock method [21], the Vlasov equation [22], or a hydrodynamical equation [23]. Our findings are based on detailed calculations using the nuclear BUU transport theory and on qualitative hydrodynamical arguments. The new torus shape is found because of memory effects from the initial stage of the collision, which are not contained in the former approaches [24]. As observable consequences we predict an increased production of intermediate-mass fragments and an additional reduction of the Coulomb barrier in the energy spectra of these fragments.

One of us (W.B.) would like to thank J. P. Bondorf and L. G. Moretto for interesting discussions which led to this investigation. This work was funded in part by the National Science Foundation Grant No. PHY 90-17077. W.B. acknowledges a Presidential Faculty Fellow award.

- 
- [1] J. Hüfner, Phys. Rep. **125**, 131 (1985).
  - [2] W. A. Friedman and W. G. Lynch, Phys. Rev. C **28**, 16 (1983); **28**, 950 (1983).
  - [3] R. W. Minich *et al.*, Phys. Lett. **118B**, 458 (1982); A. S. Hirsch *et al.*, Phys. Rev. C **29**, 508 (1984).
  - [4] J. P. Bondorf, Nucl. Phys. **A387**, 25c (1982).

- [5] J. Randrup and S. E. Koonin, Nucl. Phys. **A356**, 223 (1981).
- [6] D. H. E. Gross *et al.*, Z. Phys. A **309**, 41 (1982).
- [7] P. J. Siemens, Nature (London) **305**, 410 (1983).
- [8] M. W. Curtin, H. Toki, and D. K. Scott, Phys. Lett. **123B**, 289 (1983).
- [9] L. P. Csernai and J. I. Kapusta, Phys. Rep. **131**, 223 (1986).
- [10] W. Bauer *et al.*, Phys. Lett. **150B**, 53 (1985); Nucl. Phys. **A452**, 699 (1986); W. Bauer, Phys. Rev. C **38**, 1297 (1988).
- [11] X. Campi, Phys. Lett. B **208**, 351 (1988).
- [12] G. F. Bertsch, H. Kruse, and S. Das Gupta, Phys. Rev. C **29**, 673 (1984); G. F. Bertsch and S. Das Gupta, Phys. Rep. **160**, 189 (1988).
- [13] H. Stöcker and W. Greiner, Phys. Rep. **137**, 277 (1986).
- [14] W. Bauer *et al.*, Phys. Rev. C **34**, 2127 (1986); W. Bauer, Phys. Rev. Lett. **61**, 2534 (1988); W. Bauer, C. K. Gelbke, and S. Pratt, Annu. Rev. Nucl. Part. Sci. **42**, 77 (1992).
- [15] G. F. Bertsch and P. J. Siemens, Phys. Lett. **126B**, 9 (1983).
- [16] C. J. Pethick and D. G. Ravenhall, Nucl. Phys. **A471**, 19c (1987).
- [17] C. Ngô *et al.*, Nucl. Phys. **A499**, 148 (1989).
- [18] W. Bauer, G. F. Bertsch, and S. Das Gupta, Phys. Rev. Lett. **58**, 863 (1987).
- [19] L. G. Moretto *et al.*, Report No. LBL-31812, 1992 (to be published).
- [20] L. Phair and W. Bauer (to be published).
- [21] A. Dhar and S. Das Gupta, Phys. Rev. C **30**, 1545 (1984).
- [22] L. Vinet *et al.*, Nucl. Phys. **A468**, 312 (1987).
- [23] J. Nemeth *et al.*, Z. Phys. A **323**, 419 (1987).
- [24] Following an idea of J. A. Wheeler, C. Y. Wong has studied the possible occurrence of superheavy toroidal nuclei in a liquid drop model: Phys. Lett. **41B**, 446 (1972); and Ann. Phys. (N.Y.) **77**, 279 (1973).